Mathew Jessop-Fabre ORCID iD: 0000-0001-7534-2230

Mathias Biron ORCID iD: 0000-0002-2952-9763

The transcriptome and flux profiling of Crabtree-negative hydroxy acid producing strains of *Saccharomyces cerevisiae* reveals changes in the central carbon metabolism

Mathew M Jessop-Fabre[1]

Jonathan Dahlin[1]

Mathias B Biron[1]

Vratislav Stovicek[1]

Birgitta E Ebert[2]

Lars M Blank[2]

Itay Budin[5]

Jay D Keasling[1,3,4,5,6]

Irina Borodina[1]

[1] The Novo Nordisk Foundation for Biosustainability, Technical University of Denmark, Building 220, 2800 Kongens Lyngby, Denmark

[2] Institute of Applied Microbiology, RWTH Aachen University, Worringer Weg 1, 52056 Aachen, Germany

[3] Joint BioEnergy Institute, Emeryville, CA, USA

[4] Biological Systems & Engineering Division, Lawrence Berkeley National Laboratory, Berkeley, CA, USA

This article has been accepted for publication and undergone full peer review but has not been through the copyediting, typesetting, pagination and proofreading process, which may lead to differences between this version and the Version of Record. Please cite this article as doi: 10.1002/biot.201900013.

[5] Department of Chemical and Biomolecular Engineering & Department of Bioengineering University of California, Berkeley, CA, USA

[6] Center for Synthetic Biochemistry, Institute for Synthetic Biology, Shenzhen Institutes for Advanced Technologies, Shenzhen, China

Correspondence: Dr. Irina Borodina, The Novo Nordisk Foundation for Biosustainability, Technical University of Denmark, Building 220, 2800 Kongens Lyngby, Denmark.

E-mail: irbo@biosustain.dtu.dk

Keywords: Transcriptomics, ^{13}C-based metabolic flux analysis, hydroxy acid, central carbon metabolism, Crabtree-negative

Abbreviations: PDC, pyruvate decarboxylase; **3HP,** 3-hydroxypropionic acid; **HIBADH**, 3-hydroxyisobutyrate dehydrogenase; **HPDH,** 3-hydroxypropionate dehydrogenase

Abstract

Saccharomyces cerevisiae is a yeast cell factory of choice for the production of many bio-based chemicals. However, it is also a Crabtree-positive yeast and so it shuttles a large portion of carbon into ethanol, even under aerobic conditions. To minimise the carbon loss, ethanol formation can be eliminated by deleting pyruvate decarboxylase (PDC) activity. Deletion of PDC genes has a profound impact on *S. cerevisiae* physiology, and it is not yet well understood how PDC-negative yeasts are affected when engineered to produce other products than ethanol.

In this study, we introduced pathways for the production of three hydroxy acids (lactic, malic, or 3-hydroxypropionic acid) into an evolved PDC-negative strain. We characterised these strains *via* transcriptome and flux profiling to elucidate the effects that the production of these hydroxy acids has on the host strain. The expression of lactic acid and malic acid biosynthesis pathways improved the maximum specific growth rate (μ_{max}) of the strain by 64 and 20% respectively, presumably due to NAD^+ regeneration. On the contrary, the 3HP pathways expression decreased the μ_{max}. All strains showed a very high flux (>90% of

glucose uptake) into the oxidative pentose phosphate pathway under batch fermentation conditions. The transcriptional profile was least affected by the production of lactic acid and more by malic or 3-hydroxypropionic acids.

The study, for the first time, directly compares the flux and transcriptome profiles of several different hydroxy acid producing strains of an evolved PDC-negative *S. cerevisiae* and suggests directions for future metabolic engineering.

Graphical Abstract

Yeast Saccharomyces cerevisiae holds great potential as a host organism for the industrial production of organic acids, an industrially relevant class of chemicals. In this work, the authors investigated metabolic fluxes and transcriptional profiles of Crabtree-negative yeast strains engineered to produce three different hydroxy acids. The results provide guidance for further improvement of hydroxy acid production in yeast.

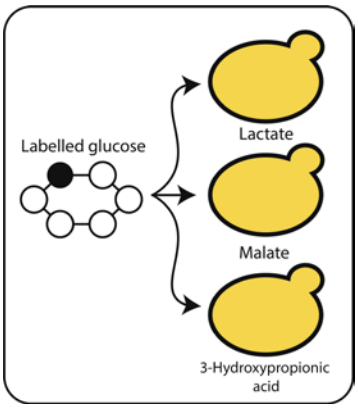

1 Introduction

Saccharomyces cerevisiae has long been used as a production organism for ethanol and more recently other biochemicals and recombinant proteins. When grown on high concentrations of glucose, yeast ferments and produces ethanol even in abundant oxygen conditions [1]. This is known as the Crabtree effect, and while such a trait has proven useful for ethanol fermentation, the alcohol is an unwanted by-product in the bio-based production of many other chemicals [2–4]. Under fermentative growth on glucose, a large fraction of the flux from pyruvate passes through the three main pyruvate decarboxylases (PDC) to be converted into

acetaldehyde, which is in turn reduced to ethanol *via* alcohol dehydrogenases (ADH), with Adh1p as the major ADH isozyme [5]. Pyruvate decarboxylase activity is conferred through the three major PDC isozymes; Pdc1p, Pdc5p, and Pdc6p [6–8]. One successful strategy for the removal of ethanol formation has been to eliminate pyruvate flux into acetaldehyde by deleting all three major PDC isozymes [4,9]. Such a PDC-negative strain is hyper-sensitive to glucose and cannot grow on high concentrations of glucose without the addition of a C2 compound such as ethanol or acetate [10]. The growth defect is caused by a redox co-factor imbalance, where NADH generated during glycolysis can no longer be oxidized during ethanol formation, and by the lack of cytosolic acetyl-CoA, which is synthesized from acetaldehyde via acetate. Previously, directed evolution of a PDC-negative strain eliminated its dependency on C2 compounds, and greatly improved its glucose tolerance and growth characteristics [11]. While some of the wild-type (WT) growth characteristics were rescued, the resulting strain (referred to as the TAM strain) still has a much slower growth rate than WT; 0.20 h^{-1} vs. 0.33 h^{-1} [11]. The genome of the TAM strain was later sequenced, revealing that much of the observed phenotype was due to a large deletion in the glucose-sensing transcriptional regulator *MTH1* [12]. This deletion is hypothesised to reduce the degradation rate of Mth1p. Mth1p reduces the expression of hexose kinase-coding genes and slows down glucose uptake rate, which in turn reduces the redox co-factor imbalance caused by NADH generation during glycolysis [12]. The reduction in glucose uptake presumably also leads to de-repression of the *ACH1* gene, encoding a mitochondrial protein with CoA transferase activity. Ach1p generates acetate from acetyl-CoA in mitochondria. Acetate can cross the mitochondrial membrane to enter the cytosol, where it is activated into acetyl-CoA, providing this compound that is essential for cell growth. The TAM strain is a pyruvate over-producer and an attractive host for the production

of pyruvate-derived chemicals, such as industrially important hydroxy acids: malic, lactic, and 3-hydroxypropionic acids [11,13–16]. In the present study, we characterised these three different hydroxy acid production pathways and the impact of the added pathways on the metabolism and physiology of the host TAM strain.

Lactic acid, a three carbon α-hydroxy acid, can be produced from pyruvate in a single enzymatic step by lactate dehydrogenase (LDH) with NADH as the cofactor. This enzyme, most commonly taken from *Lactobacillus* origin, has been shown to produce high levels of lactate in both PDC-positive and PDC-negative *S. cerevisiae* strains [13,17–20]. The TAM strain has a redox imbalance due to NAD+ not being regenerated through the formation of ethanol. The addition of the *Lactobacillus plantarum ldh1* gene in a PDC-negative strain can provide the cell with NAD+, re-balancing the redox state of the cell (Figure 1). However, this redox balancing has been shown to not be able to recover anaerobic growth, with lactic acid production being highly dependent on oxygen availability [18]. Lactic acid transport, unlike ethanol, is assumed to be dependent on ATP, and is less efficient under anaerobic conditions where ATP production is limited [18,21].

High levels of malic acid, a four-carbon α-hydroxy acid, can be produced by overexpression of three genes. The overexpression of the native pyruvate carboxylase gene *PYC1*, the native NADH-dependent malate dehydrogenase *MDH3* lacking the peroxisomal targeting sequence [22], and the malate transporter from *Schizosaccharomyces pombe MAE1*, allows for high malate titres when expressed in the TAM strain, of up to 59 g L^{-1} [16]. This pathway also regenerates NAD+, but is more energetically demanding than the lactic acid pathway because, in addition to the ATP required for malic acid export, ATP is also used for the carboxylation of pyruvate into oxaloacetate [14,23,24]. The export energetics are also different between monocarboxylic and dicarboxylic acids, and export of malic acid may have a

greater total ATP requirement than lactic acid export [14]. Addition of calcium carbonate has been shown to greatly increase malate titres through its ability to prevent product inhibition [25].

The three carbon β-hydroxy acid, 3-hydroxypropionic acid (3HP), can be produced *via* β-alanine – a pathway identified as having a high potential for 3HP production [26]. This pathway in a PDC-positive *S. cerevisiae* strain showed titres close to 14 g L^{-1} in controlled bioreactor fermentations [15]. Five enzymatic steps are required to produce 3HP from pyruvate, three of which require heterologous genes (Figure 1). The final step in this pathway, the conversion of malonic semialdehyde to 3HP, can be performed either by a 3-hydroxyisobutyrate dehydrogenase (HIBADH) that uses NADH as cofactor or a 3-hydroxypropionate dehydrogenase (HPDH) that uses NADPH. In this study, we compared both the HIBADH- and HPDH-based pathways for 3HP biosynthesis.

2 Materials and methods

2.1 Strains

Escherichia coli DH5α was used to clone, propagate, and store the plasmids. A derivative of *S. cerevisiae* strain CEN.PK, the TAM strain, was a kind gift of Prof. Jack Pronk and was used as the host strain for the hydroxy acid production strains (Delft Technical University, Holland). A description of each strain used in this study is shown in Table 1. For the respiration experiments, the CEN.PK113-7D PDC-positive strain (*MATa URA3 HIS3 LEU2 TRP1 MAL2-8c SUC2*) was used as reference. This was a kind gift from Peter Kötter, Johann Wolfgang Goethe University, Frankfurt, Germany.

2.2 Plasmid construction and yeast transformation

Each of the plasmids (Table S2) used to create the hydroxy acid producing strains (Table S3) were constructed using the EasyClone vector set for chromosomal gene integrations with auxotrophic selection markers as described in [27]. Yeast promoter biobricks were

amplified from the genomic DNA of CEN.PK113-7D *via* PCR, using primer overhangs (Table S1) for cloning as described in [27]. STlac_7031 was built with the insertion of the *Lactobacillus plantarum ldh1* (Table S4) under the control of the native *TDH3* promoter for the conversion of pyruvate to lactate. Strain STmal_5413 was constructed from the TAM strain with the insertion of *MDH3* lacking the SKL mitochondrial targeting sequence (Table S4), under control of the *TDH3* promoter. This gene was amplified from the genomic DNA of *S. cerevisiae* with primers PR7011 and PR7012 to amplify the region lacking the mitochondrial targeting sequence. The *S. pombe* malate transporter gene *mae1* (Table S4) was also inserted under the control of the native *TEF1* promoter, along with the native *PYC1* and *PYC2* genes under the control of the native *TEF1* and *PGK1* promoters, respectively. SThpdh_2779 and SThibadh_2780 were engineered for 3HP production, following the designs described in [15]. Native *PYC1* and *PYC2* genes were overexpressed (under the control of the *TEF1* and *PGK1* promoters), along with the aspartate-1-dehydrogenase gene (*panD*) from *Tribolium castaneum* under the control of the *TEF1* promoter, and the β-alanine-pyruvate amino transferase (BAPAT) from *Bacillus cereus* (*yhxA*) under the control of the *TEF1* promoter. For the final enzymatic step of the 3HP biosynthetic pathway in SThpdh_2779, a 3-hydroxypropionate dehydrogenase (HPDH) from *E. coli* (*ydfG*) that uses NADPH as cofactor was expressed under the control of the *PGK1* promoter. For SThibadh_2780, an NADH-dependent 3-hydroxyisobutyrate dehydrogenase (HIBADH) from *Pseudomonas putida* (*hibdh*) was inserted, under the control of the *PGK1* promoter. Heterologous genes were codon optimised and synthesised by GeneArt (Thermo Fisher Scientific, USA). The sequences of these genes can be found in the supplementary materials. Details and sequences of the genes used to create the 3HP strains can be found in [15]. PCR amplification was performed on each gene, using the primers as described in Table S1 with corresponding primer overhangs to be compatible with the promoter biobricks [27].

The amplified promoters and genes were USER-cloned into EasyClone vectors (details of which are given in the supplementary materials) digested with SfaAI (Thermo Scientific, USA) and Nb.BsmI (New England Biolabs, USA) [27]. USER cloning (New England Biolabs, USA) was performed as previously reported, and cloned plasmids were transformed into the *E. coli* cloning strain DH5α *via* heat shock at 42 ˚C for 1 minute [27,28]. Cells were plated on lysogeny broth (LB) agar plates with 100 µg ml^{-1} ampicillin and incubated at 37 ˚C overnight. The next day, individual colonies were tested by PCR for the correctly sized plasmid insertions using the verification primers outlined in the supplementary materials. Correctness of all plasmid sequences was additionally confirmed by Sanger sequencing. Correct *E. coli* clones were stored as glycerol stocks at -80 ˚C and used for plasmid propagation.

Plasmids for yeast transformations were first digested with NotI (Thermo Scientific, USA) to produce linear DNA fragments. The fragments containing expression cassettes and selection marker flanked by homologous recombination arms were purified from the vector backbone by gel electrophoresis followed by band excision and gel purification. All yeast transformations were carried out using the lithium acetate chemical transformation protocol as described in [29]. After heat shock, the cells were plated directly onto synthetic drop-out agar plates. After 2-3 days, plates were examined for growth, and correct isolates were identified *via* PCR on individual colonies using the verification primers outlined in [27].

Complete lists of strains, plasmids, biobricks, and primers used in this study are included in the supplementary materials.

2.3 Media

For selection of *E. coli*, LB agar plates were made to contain 100 µg mL^{-1} ampicillin. For plasmid propagation, LB broth was used with the same concentration of ampicillin.

To select for *S. cerevisiae* transformants and for strain recovery from glycerol stocks, SC agar plates were prepared with pre-mixed amino acid drop-out powders, with a final

glucose concentration of 20 g L^{-1}. For the creation of pre-cultures, liquid SC media was prepared with pre-mixed amino acid drop-out powders, also with a final glucose concentration of 20 g L^{-1}. For the respiration experiments, liquid complete synthetic mixture (CSM) was prepared from drop-out powders purchased from Sunrise Science (USA), with 20 g L^{-1} glucose.

S. cerevisiae shake flask fermentations were performed with batch production medium optimised for acid production, prepared according to [16], with 100 g L^{-1} glucose as the carbon source.

2.4 Cultivation conditions

For shake flask fermentation experiments, single colonies of each strain were taken from plates and inoculated into 5 mL of liquid SC medium with appropriate amino acid selection in 12 mL culture tubes and incubated at 30°C, 250 rpm for 2 days. Shake flasks were prepared as follows; 5 g $CaCO_3$ was added to each 500 mL baffled shake flask before the flasks were autoclaved. Once cool, 100 mL of the sterile batch production medium was added to each shake flask. The prepared flasks were inoculated from the pre-cultures to a starting OD_{600} of 0.5. Fermentations were carried out at 30 ˚C, and shaking set to 250 rpm, for 5 days with samples taken every ~12 hrs and measured for optical density at 600 nm in an Implen P300 spectrophotometer (dilutions were made to keep measurements within the linear range of the equipment). Part of each sample was centrifuged at 11,000 x g for 5 min, and the supernatant was stored at -20°C until HPLC analysis. Each strain was fermented in triplicate in a shaking incubator for 120 hrs at 30 ˚C and 250 rpm.

2.5 ^{13}C-based metabolic flux analysis

For ^{13}C-based metabolic flux analysis (MFA), the same medium was used as in the shake flask fermentations, except that ammonia was used as the nitrogen source instead of urea, no $CaCO_3$ was added (to prevent non-labelled carbon interference), and ^{13}C-labelled glucose was used to a final concentration of 10 g L^{-1}. 250 mL shake flasks were filled with 10 mL of medium and inoculated with the strains to a starting OD_{600} of 0.06. Samples for

analysis were taken once the OD_{600} of the cells had reached 2.00. 0.3 mg CDW was removed and washed in 0.9% NaCl before storage at -80 ˚C. Each strain was cultured in quadruplicate, with one culture grown on 20% U-^{13}C and 80% unlabelled glucose, and the three other cultures grown on 20% U-^{13}C and 80% 1-^{13}C glucose, as previously reported [30]. Labelled glucose was purchased from Eurisotop (France). The same cultivation was performed in triplicate without labelled glucose, where samples were taken regularly during growth and measured by HPLC for the rates of secreted products, used to constrain the stoichiometric model for metabolic flux analysis.

The frozen cell pellets were resuspended in 150 µl HCL (6M) before being transferred to a silanized glass vial. The samples were left to hydrolyse at 105 ˚C for 6 hrs, before the remaining liquid was evaporated at 80 ˚C. The pellets were resuspended in 30 µl acetonitrile. Derivatisation was performed by adding N-methyl-N-tert-butyldimethylsilyl-trifluoroacetamide to a final ratio of 1:1, and incubating at 85 ˚C for 1 hr [31]. GC-MS analysis of the amino acid content was performed on the derivatised samples as previously reported using a TSQ 8000 XLS Triple-Quadrupole MS equipped with a PTV-injector (Thermo-Fisher Scientific) [30].

The raw GC-MS data were corrected by the iMS2Flux (v7.2.1) software with default settings [32] for natural abundance of heavy isotopes and unlabelled biomass introduced with the inoculum. Steady-state metabolic flux analysis was then performed with the INCA (v1.6) toolbox for MATLAB R2016b [33]. A previously reported model metabolic network for *S. cerevisiae* was adjusted to fit the central carbon metabolism of each acid producing strain and used as the model network input for INCA [34]. The full list of included reactions is included in the supplementary information (Table S5). Glyoxylate cycle reactions were not included in the metabolic model due to the negligible activity when glucose is used as a substrate. Flux estimation was performed 10 times with randomised initial guesses, and goodness-of-fit was assessed. The minimized residual sum

of squares for each experiment was below 300. 95 % confidence intervals of the flux parameters were calculated using the Monte Carlo method in INCA.

The metabolic fluxes estimated with INCA were used to constrain a modified version of the iMM904 genome scale metabolic model (GEM) of *S. cerevisiae* [35]. This model was modified by deleting the PDC reaction to eliminate ethanol production, and the heterologous pathways for each strain were added to the reactions in the model, producing a distinct model for each strain. These models were used to determine the remainder of the fluxes using parsimonious flux balance analysis (pFBA) implemented in the Cameo (v0.11.6) toolbox for Python 3.4 [36,37].

2.6 Transcriptomics

For transcriptomic analysis, triplicate fermentations identical to those for the ^{13}C-MFA experiments were performed with non-labelled glucose. Once the fermentations reached the harvest OD_{600} of 2, biomass samples were removed, cooled quickly on ice, and centrifuged at 4 ˚C for 10 mins at 5,000 x g. The supernatant was removed, the pellets were snap-frozen with liquid nitrogen and stored at -80 ˚C until they were further processed. For RNA extraction, the RNeasy mini kit (Qiagen) was used, followed by treatment with DNase (RNase-Free DNase Set, Qiagen) for the digestion of residual genomic DNA. Library preparation and sequencing was performed as described previously [30]. Mapping, alignment, and differential expression analysis were performed with the HISAT2 (v2.1.0), StringTie (v1.3.5), and DESeq. 2 (v1.22.1) in R Studio (v1.1.442) [38–40]. The false discovery rate for differential expression was controlled for by the Benjamini-Hochberg method, after p-value estimation *via* the Wald significance test [39,41]. Principle component analysis (PCA) was performed with the PCA tools within DESeq. 2. Array Express accession number: E-MTAB-7600.

2.7 Analytical methods

Concentrations of extracellular metabolites were measured by HPLC. The supernatant was removed and transferred to Nunc 96-well plates with rubber sealing top (Thermo Scientific, USA). 30 µL of each sample were injected and analytes separated on an Aminex HPX-87H ion exclusion column (Bio-Rad, USA) at 60°C using 5 mM H_2SO_4 was used as eluent with a flow rate of 600 µL min^{-1} for 30 min. The compounds were detected with a Dionex RI-101 Refractive Index Detector at 45°C and an DAD-3000 Diode Array Detector at 210 nm (Dionex, USA). For analysis of 3HP, the same protocol was run except that 1 mM H_2SO_4 was used as eluent, with a longer run time of 45 minutes. Due to the overlapping spectra of pyruvate and malate in this method, malate concentrations were verified using the L-malic acid assay kit (K-LMAL-116A, Megazyme, Republic of Ireland). Pyruvate was verified using a pyruvic acid assay kit (K-PYRUV, Megazyme, Republic of Ireland). Standards for analysis were purchased from Sigma Aldrich, USA. The 3HP standard was purchased from TCI, Japan.

2.8 Respiration monitoring

To analyse the respiration characteristics of the hydroxy acid production strains, each strain was tested in a respiration activity monitoring system (RAMOS) [42]. Individual colonies of each strain were inoculated into 5 mL of CSM lacking the appropriate amino acids. The following day the RAMOS was calibrated and checked for correct function following the manufacturer guidelines. The RAMOS shake flasks were inoculated to a starting OD_{600} of 0.2 and set to shake at 300 rpm with the temperature set to remain constant at 30°C. The fermentations lasted for 48 hrs, with oxygen and carbon dioxide automatically measured every 30 mins. Samples were taken for analysis and tested for optical density every ~12 hrs. Each experiment was performed in triplicate.

2.9 Statistics

The fermentation data in this study were analysed, and statistics calculated using GraphPad Prism software version 7 (GraphPad Software, Inc.). Significance was calculated with Tukey's multiple comparisons test for one-way ANOVA. All values are expressed as the mean average ± standard deviation.

2.10 Chemicals

Unless otherwise stated, all reagents and chemicals were purchased from Sigma-Aldrich, USA.

3 Results

3.1 Physiological characterization of hydroxy acid producing PDC-negative *S. cerevisiae*

We constructed four different hydroxy acid producing strains, all with an evolved glucose-tolerant PDC-negative strain as the chassis – referred to as the TAM strain, which produces and excretes high levels of pyruvate [11]. We chose three different hydroxy acids that are commonly produced from pyruvate; lactic, malic, and 3HP acid. We reconstructed previously published designs for high level production of lactate, and malate with the TAM strain [16,43]. Two different versions of the β-alanine route to 3HP biosynthesis were constructed, each utilising a different redox cofactor (NADH or NADPH) in the final enzymatic step of the pathway [15].

We performed shake flask fermentations using a batch medium composition that has previously been shown to be suitable for the production of malic acid to high titres in the TAM strain. 100 g L^{-1} of glucose was used as the carbon source, with 50 g L^{-1} $CaCO_3$ added as a neutralising agent (Figure 2, Table 1) [16]. Growth rates, under this condition, were similar for all of the strains apart from for the lactate producer (STlac_7031) which had a significantly ($p < 0.01$) higher growth rate (0.094±0.016) than the parental strain STtam_2803 (0.057±0.004 h^{-1}).

STlac_7031 and STmal_5413 both produced high levels of their products, with final measured lactate and malate concentrations of 30.2±2.2, and 26.8±0.3 g L^{-1} respectively. This was higher than the pyruvate production in the parental strain, which had a maximum titre of only 16.5±0.1 g L^{-1}. SThpdh_2779 and SThibadh_2780 showed continued product formation into stationary phase. The two 3HP strains produced similar levels of 3HP by the end of the fermentation, 3.7±0.13, and 3.4±0.17 g L^{-1} respectively. STtam_2803 produced high levels of glycerol, with ~6 g L^{-1} measured after 120 hours. Glycerol production was lower in all of the other strains. The final C-mol yield of lactate in STlac_7031 was 25%, greater than that of malate in ST5314 (0.30 *vs.* 0.24 C-mol C-mol^{-1} glucose), potentially due to the lower energetic requirement of lactate biosynthesis. Differences in by-product secretion were found between the two 3HP producing strains. Both produced similar levels of succinate (~0.8 g L^{-1}), but SThibadh_2780 produced 50% more glycerol than SThpdh_2779 (3 g L^{-1} and 2 g L^{-1} respectively).

3.2 Characterisation of respiration profiles

The respiration activity monitoring system (RAMOS) is capable of measuring both the oxygen and carbon transfer rates (OTR and CTR) during microbial fermentations, and from this determine the respiratory quotients (RQ) of the strains [42]. STtam_2803 showed a tightly linked OTR and CTR through the fermentations, with an RQ of 1. All of the tested strains had near identical OTRs during the first 10 hours of fermentation. STlac_7031 was the PDC-negative strain showing the earliest slow-down of OTR, beginning at ~18 hours (Supplementary Figure S1). However, later in the fermentation, the OTR of STlac_7031 raised again and showed two additional peaks not observed in any of the other experiments. The cause of this profile is not precisely clear, but it could be due to the consumption of pyruvate and/or lactate after the glucose has been depleted [44]. Additionally, STlac_7031, similar to the PDC-positive strain, was able to metabolise all of the glucose with lower levels of total oxygen consumption compared to the other strains (supplementary information).

3.3 ^{13}C-based metabolic flux analysis

We employed ^{13}C-based metabolic flux analysis, combined with genome-scale modelling to identify flux distribution differences between the production strains. Each strain was cultivated in defined liquid batch medium containing 10 g/L of ^{13}C-labelled glucose as the carbon source [16]. The strains were cultivated in shake flasks lacking $CaCO_3$, and samples taken when each strain reached mid-exponential phase. Once collected, samples were analysed by GC-MS and the fluxes were calculated using the iMS2flux, and INCA programs [32,33]. The iMM904 genome-scale model of *S. cerevisiae* was constrained with the calculated fluxes to estimate the global flux distribution for each strain (Figure 3).

Using the medium without $CaCO_3$resulted in higher maximum specific growth rates μ_{max} of the strains than in the previous cultivations with 100 g/L and $CaCO_3$ in section 3.1 (Table S6). STlac_7031 and STmal_5413 strains had respectively 64 and 20% higher μ_{max} than STtam_2803, while both 3HP-producing strains showed 21-26% lower rates than STtam_2803. In the Table S6, the secretion rates of metabolites are also presented. We succeeded in quantifying pyruvate in these cultivations using an enzymatic assay. Interestingly, pyruvate secretion rates were much lower in STlac_7031 (0.131 ± 0.016 mmol $gCDW^{-1}$ h^{-1}) and STmal_5413 (0.130 ± 0.026 mmol $gCDW^{-1}$ h^{-1}) strains than in the parental STtam_2803 strain (0.541 ± 0.106 mmol $gCDW^{-1}$ h^{-1}), while pyruvate secretion rates for the 3HP-producing strains were not significantly different from the parent strain.

During respiro-fermentative growth, as is expected during shake flask cultivations, fluxes through the pentose phosphate (PP) pathway and TCA cycle are typically low in PDC-positive WT strains [45,46]. In contrast, all PDC-negative strains analysed in the present study diverted most of the carbon flux (>90%) into the PP pathway. However, in a previous MFA study of a malate producing variant of the TAM background, such a high flux into the PP pathway was not observed [16]. Differences in the experimental conditions and methods of analysis between the two studies may explain some of the

variation, but further work is required to identify the cause of the high carbon flux in the PP pathway in the strains presented here. The flux through the TCA cycle remained low, especially in both 3HP producing strains.

Both 3HP strains showed higher relative fluxes compared with STlac_7031 and STmal_5413 (but lower than the parental strain) into glycerol-3-phosphate from DHAP, and from the reversed transaldolase reaction: E4P + F6P -> S7P + G4P. STlac_7031 and STmal_5413 kept a high proportion of their carbon flux through 3-phosphoglycerate to pyruvate, presumably due to the presence of a suitable carbon sink. From pyruvate, both 3HP strains showed flux ratios similar to STmal_5413 for oxaloacetate synthesis. SThibadh_2780 showed higher pyruvate carboxylase flux than SThpdh_2779, but both strains showed near identical fluxes through the aspartate amino transferase step, with the reaction only processing around half of the flux supplied from the pyruvate carboxylase reaction (supplementary information).

3.4 Transcriptome analysis

We performed an analysis of the transcriptomes of the hydroxy acid production strains to probe how the introduced pathways affect the transcriptional profile (Figure 3). STlac_7031 displayed nine transcripts that were significantly ($q<0.05$) and highly differentially expressed (± 2-fold change), while STmal_5413 displayed 41 such transcripts, SThpdh_2779 had 23, and SThibadh_2780 had 30 (all in comparison with the TAM strain). A total of 69 highly differentially expressed transcripts were found across the strains, but none were found to be highly differentially expressed across all strains. A total of seven transcripts were highly differentially expressed across the three strains (*IRT1, YAR075W, HSP26, PAU15, DED1, YPR145C-A, YMR175W-A*). Several of these encode proteins of unknown function, but characterized transcripts are involved in a diverse set of cellular functions; including control of gametogenesis, heat-shock response, and translation initiation. Out of the 23 genes that were highly differentially expressed in SThpdh_2779, 18 of these were also found in SThibadh_2780. Several genes involved in

the allantoin degradation pathway were found to be highly upregulated, which was also observed in a PDC-positive strain expressing the β-alanine pathway (unpublished results). We analysed the variance across the strains *via* principle component analysis (PCA), as shown in Figure 4. This illustrates that STlac_7031 only showed a small variance from the parental STtam_2803, while STmal_5413 showed higher variation from STtam_2803, as did SThpdh_2779 and SThibadh_2780. These latter two strains showed a small variation from one another and both were discrete from the profile of STmal_5413.

We next mapped the transcriptional profiles to central carbon metabolism (Figure 3). STlac_7031 showed only slight differences in transcript levels over the central carbon metabolism, with small changes in the genes involved in glycerol production. The remaining strains showed greater deviation in their transcriptional abundances. STmal_5413, SThpdh_2779, and SThibadh_2780 all upregulated *HXK2*, a gene involved in the conversion of glucose to glucose-6-phosphate, the flux-controlling step of glycolysis. STlac_7031 also showed an upregulation of this step, but instead through *GLK1*. However, only STmal_5413 and STlac_7031 showed higher glucose uptake rates than the parental strain (Table S5). STmal_5413, SThpdh_2779, and SThibadh_2780 all showed downregulation across parts of the pentose phosphate pathway and in steps found in lower glycolysis. While TCA cycle genes did not show large transcriptional changes, STmal_5413 experienced upregulation of the two steps required to convert citrate to α-ketoglutarate, while SThpdh_2779 and SThibadh_2780 experienced upregulation of *FUM1*, responsible for fumarate to malate conversion.

4 Discussion

In this study, we characterised hydroxy acid production in a Crabtree-negative, pyruvate overproducing *S. cerevisiae* strain – the TAM strain. Introduction of a lactate or malate production pathway restores some of the growth defects found in the TAM strain by re-supplying cytosolic NAD+. The energetic requirements of lactate and malate transport,

combined with the mutation found in *MTH1*, prevents STlac_7031 and STmal_5413 from reaching the growth rate of ethanol-producing PDC-positive *S. cerevisiae*. Interestingly, although lactate production facilitated a significantly higher growth rate in STlac_7031, the transcriptional profile remained close to that of the parental strain, suggesting that this pathway has not caused a dramatic shift in the regulatory mechanisms of the TAM strain. Malate production does appear to cause large changes across the regulatory mechanisms, with a significant divergence in profile compared to the parental strain. Unlike lactate and malate production, NADH-dependent production of 3HP in SThibadh_2780 was unable to provide any growth restoration, and both 3HP producing strains had reduced growth rates compared to STtam_2803 when fermented in the absence of $CaCO_3$. A slight growth improvement of the HIBADH (SThibadh_2780) strain over the HPDH strain (SThpdh_2779) may have been expected due to SThibadh_2780 regenerating NAD^+ during 3HP synthesis, but no such difference between the strains was observed. Both strains showed similar transcriptional profiles across central carbon metabolism, and no difference between them was observed in the NADPH producing PP pathway, of which both strains down-regulated several genes. The lower growth rates suggest that both 3HP pathways are deleterious to the fitness of the host, perhaps due to the accumulation of 3-hydroxypropionic aldehyde [47]. This effect, together with the much lower titres of 3HP compared to the other hydroxy acids, may cancel any positive effects provided by NAD^+ regeneration.

Pyruvate yields on glucose were reported in the TAM strain to be 0.92 mol mol^{-1} glucose [11]. In this study we record yields of only 0.34 mol mol^{-1} glucose. This difference is most likely due to the repeated glucose feedings used in the previous report. We also obtained lower yields for lactate and malate production (0.60 mol mol^{-1} *vs.* 1.44 mol mol^{-1} glucose for lactate production, and 0.36 *vs.* 0.42 mol mol^{-1} glucose for malate production) [16,43]. The cause of this difference is likely due to the use of high copy-number plasmids in the previous works, and only single copy chromosomal integrations in the present study. PDC-

positive *S. cerevisiae* expressing the HPDH version of the 3HP pathway produced a yield of 0.09 mol mol^{-1} glucose in batch media conditions, slightly higher than the same pathway expressed in the TAM strain – SThpdh_2779 (0.07 mol mol^{-1} glucose) [15]. The poorer performance of the TAM based strains compared to the PDC-positive host is surprising, and perhaps due to the media conditions not being optimal for 3HP production. However, the 3HP titres were much higher than those previously published under batch fermentation conditions [15]. When these 3HP pathways were expressed in a PDC-positive strain, there was a greater difference between the performance of the HPDH and HIBADH enzymes, with the strain carrying HPDH producing ~4-fold higher titres of 3HP than a strain carrying the HIBADH enzyme [15]. The observation that the HIBADH pathway performed relatively better in the TAM background is consistent with expectations as the PDC-negative strain exhibits an NADH imbalance.

Both SThpdh_2779 and SThibadh_2780 have similar fluxes into oxaloacetate as STmal_5413, suggesting that *PYC1* and *PYC2* overexpression is correctly functioning to push flux into oxaloacetate in these strains. However, they are unable to channel this additional flux into 3HP production. Even though SThibadh_2780 showed higher flux than SThpdh_2779 through pyruvate carboxylase, the near identical downstream fluxes of both strains suggest that the flux controlling step is positioned lower in the pathway. One candidate for this step is aspartate decarboxylase. We previously reported that increasing the copy number of aspartate decarboxylase encoding gene improved 3HP production in the PDC-positive background [15]. Both strains also showed similar transcriptional profiles, and both showed differentially expressed genes related to allantoin degradation. Further investigation may uncover what role this pathway may be having on 3HP production *via* this pathway.

The impaired growth of both 3HP strains may be due in part to a toxic accumulation of malonic semialdehyde, with the detoxification by HPDH/HIBADH unable to proceed quickly enough to allow the cell to grow rapidly [48,49]. Investigations of the transport

mechanisms of 3HP from the cytosol to the extracellular space could help to pull flux from malonic semialdehyde and restore growth. Another strategy may be to engineer a malonic semialdehyde sensor to dynamically control flux through the pathway, similar to previous work carried out on 3HP biosensors [50,51].

We hope that the data provided here will help to inform future attempts to engineer hydroxy acid production in PDC-negative hosts. Our findings illustrate how the fluxes are distributed in these strains, and how the different production pathways impact the transcriptional landscape. However, further work is required to identify the mechanisms behind these changes and how they may be exploited to increase the productivity of these hosts.

Acknowledgement

The authors acknowledge the financial support from the Novo Nordisk Foundation (Grant Agreement no. NNF10CC1016517), from the European Research Council under the European Union's Horizon 2020 research and innovation programme (YEAST-TRANS project, Grant Agreement no. 757384), from the European Commission in the 7th Framework Programme (BioREFINE-2G project, Grant Agreement no. FP7-613771), and from the European Union's Horizon 2020 research and innovation programme under the Marie Skłodowska-Curie grant agreement No 722287 (PaCMEN project). MJ-F thanks the Idella foundation for financing the research stay at Joint BioEnergy Institute, USA. LMB acknowledges funding by the Cluster of Excellence "The Fuel Science Center - Adaptive Conversion Systems for Renewable Energy and Carbon Sources", which is funded by the Excellence Initiative of the German federal and state governments to promote science and research at German universities.

We thank Prof. Jack Pronk (TU Delft) for the gift of S. cerevisiae TAM strain and Prof. Peter Kötter, Johann Wolfgang Goethe University, Frankfurt, Germany for the gift of the S. cerevisiae strain CEN.PK113-7D.

Conflict of interest

IB has a financial interest in BioPhero ApS. JDK has a financial interest in Amyris, Lygos, Demetrix, Constructive Biology, Maple Bio, Ansa Biotechnology, and Napigen.

5 References

[1] J.T. Pronk, H. Yde Steensma, J.P. Van Dijken, Pyruvate metabolism in Saccharomyces cerevisiae., Yeast. 12 (1996) 1607–1633. doi:10.1002/(SICI)1097-0061(199612)12:16<1607::AID-YEA70>3.0.CO;2-4.

[2] S. Kim, J.-S. Hahn, Efficient production of 2,3-butanediol in Saccharomyces cerevisiae by eliminating ethanol and glycerol production and redox rebalancing, Metab. Eng. 31 (2015) 94–101. doi:https://doi.org/10.1016/j.ymben.2015.07.006.

[3] E. Nevoigt, Progress in Metabolic Engineering of Saccharomyces cerevisiae, Microbiol. Mol. Biol. Rev. 72 (2008) 379–412. doi:10.1128/MMBR.00025-07.

[4] M.T. Flikweert, J.P. van Dijken, J.T. Pronk, Metabolic responses of pyruvate decarboxylase-negative Saccharomyces cerevisiae to glucose excess., Appl. Environ. Microbiol. . 63 (1997) 3399–3404. http://aem.asm.org/content/63/9/3399.abstract.

[5] O. de Smidt, J.C. du Preez, J. Albertyn, The alcohol dehydrogenases of Saccharomyces cerevisiae: a comprehensive review., FEMS Yeast Res. 8 (2008) 967–978. doi:10.1111/j.1567-1364.2008.00387.x.

[6] H.D. Schmitt, F.K. Zimmermann, Genetic analysis of the pyruvate decarboxylase reaction in yeast glycolysis., J. Bacteriol. 151 (1982) 1146–1152.

[7] P.G. Seeboth, K. Bohnsack, C.P. Hollenberg, pdc1 Mutants of Saccharomyces cerevisiae Give Evidence for an Additional Structural PDC Gene: Cloning of PDC5, a Gene Homologous to PDC1, J. Bacteriol. 172 (1990) 678–685.

[8] S. Hohmann, Characterization of PDC6, a third structural gene for pyruvate decarboxylase in Saccharomyces cerevisiae., J. Bacteriol. 173 (1991) 7963–7969.

[9] M.T. Flikweert, L. van der Zanden, W.M.T.M. Janssen, H. Yde Steensma, J.P. van Dijken, J.T. Pronk, Pyruvate decarboxylase: An indispensable enzyme for growth of Saccharomyces cerevisiae on glucose, Yeast. 12 (1996) 247–257. doi:10.1002/(SICI)1097-0061(19960315)12:3<247::AID-YEA911>3.0.CO;2-I.

[10] M.T. Flikweert, M. de Swaaf, J.P. van Dijken, J.T. Pronk, Growth requirements of pyruvate-decarboxylase-negative Saccharomyces cerevisiae., FEMS Microbiol. Lett. 174 (1999) 73–79.

[11] A.J.A. van Maris, J.-M.A. Geertman, A. Vermeulen, M.K. Groothuizen, A.A. Winkler, M.D.W. Piper, J.P. van Dijken, J.T. Pronk, Directed Evolution of Pyruvate Decarboxylase-Negative Saccharomyces cerevisiae, Yielding a C2-Independent, Glucose-Tolerant, and Pyruvate-Hyperproducing Yeast, Appl. Environ. Microbiol. . 70 (2004) 159–166. http://aem.asm.org/content/70/1/159.abstract.

[12] B. Oud, C.-L. Flores, C. Gancedo, X. Zhang, J. Trueheart, J.-M. Daran, J.T. Pronk, A.J.A. van Maris, An internal deletion in MTH1 enables growth on glucose of pyruvate-decarboxylase negative, non-fermentative Saccharomyces cerevisiae, Microb. Cell Fact. 11 (2012) 131. doi:10.1186/1475-2859-11-131.

[13] N. Ishida, S. Saitoh, K. Tokuhiro, E. Nagamori, T. Matsuyama, K. Kitamoto, H. Takahashi, Efficient Production of l-Lactic Acid by Metabolically Engineered Saccharomyces cerevisiae with a Genome-Integrated l-Lactate Dehydrogenase Gene, Appl. Environ. Microbiol. . 71 (2005) 1964–1970. http://aem.asm.org/content/71/4/1964.abstract.

[14] D.A. Abbott, R.M. Zelle, J.T. Pronk, A.J.A. van Maris, Metabolic engineering of Saccharomyces cerevisiae for production of carboxylic acids: current status and challenges, FEMS Yeast Res. 9 (2009) 1123–1136. http://dx.doi.org/10.1111/j.1567-1364.2009.00537.x.

[15] I. Borodina, K.R. Kildegaard, N.B. Jensen, T.H. Blicher, J. Maury, S. Sherstyk, K. Schneider, P. Lamosa, M.J. Herrgård, I. Rosenstand, F. Öberg, J. Forster, J. Nielsen, Establishing a synthetic pathway for high-level production of 3-hydroxypropionic acid in Saccharomyces cerevisiae via β-alanine, Metab. Eng. 27 (2015) 57–64. doi:10.1016/j.ymben.2014.10.003.

[16] R.M. Zelle, E. de Hulster, W.A. van Winden, P. de Waard, C. Dijkema, A.A. Winkler, J.-M.A. Geertman, J.P. van Dijken, J.T. Pronk, A.J.A. van Maris, Malic Acid Production by Saccharomyces cerevisiae: Engineering of Pyruvate Carboxylation, Oxaloacetate Reduction, and Malate Export , Appl. Environ. Microbiol. 74 (2008) 2766–2777. doi:10.1128/AEM.02591-07.

[17] S. Colombié, S. Dequin, J.M. Sablayrolles, Control of lactate production by Saccharomyces cerevisiae expressing a bacterial LDH gene, Enzyme Microb. Technol. 33 (2003) 38–46. doi:https://doi.org/10.1016/S0141-0229(03)00082-6.

[18] A.J.A. van Maris, A.A. Winkler, D. Porro, J.P. van Dijken, J.T. Pronk,

Homofermentative Lactate Production Cannot Sustain Anaerobic Growth of Engineered Saccharomyces cerevisiae: Possible Consequence of Energy-Dependent Lactate Export, Appl. Environ. Microbiol. . 70 (2004) 2898–2905. http://aem.asm.org/content/70/5/2898.abstract.

[19] P. Branduardi, M. Sauer, L. De Gioia, G. Zampella, M. Valli, D. Mattanovich, D. Porro, Lactate production yield from engineered yeasts is dependent from the host background, the lactate dehydrogenase source and the lactate export, Microb. Cell Fact. 5 (2006) 4. doi:10.1186/1475-2859-5-4.

[20] E. Nagamori, K. Shimizu, H. Fujita, K. Tokuhiro, N. Ishida, H. Takahashi, Metabolic flux analysis of genetically engineered Saccharomyces cerevisiae that produces lactate under micro-aerobic conditions, Bioprocess Biosyst. Eng. 36 (2013) 1261–1265. doi:10.1007/s00449-012-0870-6.

[21] A. Van Maris, W. N. Konings, J. P.van Dijken, J. Pronk, Microbial export of lactic and 3-hydroxypropanoic acid: Implications for industrial fermentation processes, 2004. doi:10.1016/j.ymben.2004.05.001.

[22] L. McAlister-Henn, J.S. Steffan, K.I. Minard, S.L. Anderson, Expression and Function of a Mislocalized Form of Peroxisomal Malate Dehydrogenase (MDH3) in Yeast, J. Biol. Chem. . 270 (1995) 21220–21225. http://www.jbc.org/content/270/36/21220.abstract.

[23] C. Camarasa, F. Bidard, M. Bony, P. Barre, S. Dequin, Characterization of Schizosaccharomyces pombe Malate Permease by Expression in Saccharomyces cerevisiae , Appl. Environ. Microbiol. . 67 (2001) 4144–4151. http://aem.asm.org/content/67/9/4144.abstract.

[24] M. Casal, S. Paiva, O. Queirós, I. Soares-Silva, Transport of carboxylic acids in yeasts, FEMS Microbiol. Rev. 32 (2008) 974–994. http://dx.doi.org/10.1111/j.1574-6976.2008.00128.x.

[25] T. Zambanini, W. Kleineberg, E. Sarikaya, J.M. Buescher, G. Meurer, N. Wierckx, L.M. Blank, Enhanced malic acid production from glycerol with high-cell density Ustilago trichophora TZ1 cultivations, Biotechnol. Biofuels. 9 (2016) 135. doi:10.1186/s13068-016-0553-7.

[26] V. Kumar, S. Ashok, S. Park, Recent advances in biological production of 3-hydroxypropionic acid, Biotechnol. Adv. 31 (2013) 945–961. doi:https://doi.org/10.1016/j.biotechadv.2013.02.008.

[27] N.B. Jensen, T. Strucko, K.R. Kildegaard, F. David, J. Maury, U.H. Mortensen, J. Forster, J. Nielsen, I. Borodina, EasyClone: method for iterative chromosomal integration of multiple genes in Saccharomyces cerevisiae., FEMS Yeast Res. 14 (2014) 238–248. doi:10.1111/1567-1364.12118.

[28] H.H. Nour-Eldin, F. Geu-Flores, B.A. Halkier, USER cloning and USER fusion: the ideal cloning techniques for small and big laboratories., Methods Mol. Biol. 643 (2010) 185–200. doi:10.1007/978-1-60761-723-5_13.

[29] R.D. Gietz, R.H. Schiestl, High-efficiency yeast transformation using the LiAc/SS carrier DNA/PEG method., Nat. Protoc. 2 (2007) 31–34. doi:10.1038/nprot.2007.13.

[30] K.R. Kildegaard, N.B. Jensen, K. Schneider, E. Czarnotta, E. Ozdemir, T. Klein, J. Maury, B.E. Ebert, H.B. Christensen, Y. Chen, I.-K. Kim, M.J. Herrgard, L.M. Blank, J. Forster, J. Nielsen, I. Borodina, Engineering and systems-level analysis

of Saccharomyces cerevisiae for production of 3-hydroxypropionic acid via malonyl-CoA reductase-dependent pathway., Microb. Cell Fact. 15 (2016) 53. doi:10.1186/s12934-016-0451-5.

[31] A. Schmitz, B.E. Ebert, L.M. Blank, GC-MS-Based Determination of Mass Isotopomer Distributions for 13C-Based Metabolic Flux Analysis BT - Hydrocarbon and Lipid Microbiology Protocols: Genetic, Genomic and System Analyses of Pure Cultures, in: T.J. McGenity, K.N. Timmis, B. Nogales (Eds.), Springer Berlin Heidelberg, Berlin, Heidelberg, 2017: pp. 223–243. doi:10.1007/8623_2015_78.

[32] C.H. Poskar, J. Huege, C. Krach, M. Franke, Y. Shachar-Hill, B.H. Junker, iMS2Flux--a high-throughput processing tool for stable isotope labeled mass spectrometric data used for metabolic flux analysis., BMC Bioinformatics. 13 (2012) 295. doi:10.1186/1471-2105-13-295.

[33] J.D. Young, INCA: a computational platform for isotopically non-stationary metabolic flux analysis., Bioinformatics. 30 (2014) 1333–1335. doi:10.1093/bioinformatics/btu015.

[34] T.M. Wasylenko, G. Stephanopoulos, Metabolomic and (13)C-Metabolic Flux Analysis of a Xylose-Consuming Saccharomyces cerevisiae Strain Expressing Xylose Isomerase, Biotechnol. Bioeng. 112 (2015) 470–483. doi:10.1002/bit.25447.

[35] M.L. Mo, B.O. Palsson, M.J. Herrgard, Connecting extracellular metabolomic measurements to intracellular flux states in yeast., BMC Syst. Biol. 3 (2009) 37. doi:10.1186/1752-0509-3-37.

[36] J.G.R. Cardoso, K. Jensen, C. Lieven, A.S. Lærke Hansen, S. Galkina, M. Beber, E. Özdemir, M.J. Herrgård, H. Redestig, N. Sonnenschein, Cameo: A Python Library for Computer Aided Metabolic Engineering and Optimization of Cell Factories, ACS Synth. Biol. 7 (2018) 1163–1166. doi:10.1021/acssynbio.7b00423.

[37] N.E. Lewis, K.K. Hixson, T.M. Conrad, J.A. Lerman, P. Charusanti, A.D. Polpitiya, J.N. Adkins, G. Schramm, S.O. Purvine, D. Lopez-Ferrer, K.K. Weitz, R. Eils, R. König, R.D. Smith, B.Ø. Palsson, Omic data from evolved E. coli are consistent with computed optimal growth from genome-scale models, Mol. Syst. Biol. 6 (2010) 390. doi:10.1038/msb.2010.47.

[38] M. Pertea, D. Kim, G.M. Pertea, J.T. Leek, S.L. Salzberg, Transcript-level expression analysis of RNA-seq experiments with HISAT, StringTie and Ballgown, Nat. Protoc. 11 (2016) 1650. https://doi.org/10.1038/nprot.2016.095.

[39] M.I. Love, W. Huber, S. Anders, Moderated estimation of fold change and dispersion for RNA-seq data with DESeq. 2, Genome Biol. 15 (2014) 550. doi:10.1186/s13059-014-0550-8.

[40] D. Kim, B. Langmead, S.L. Salzberg, HISAT: a fast spliced aligner with low memory requirements, Nat. Methods. 12 (2015) 357. https://doi.org/10.1038/nmeth.3317.

[41] Y. Benjamini, Y. Hochberg, Controlling the False Discovery Rate: A Practical and Powerful Approach to Multiple Testing, J. R. Stat. Soc. Ser. B. 57 (1995) 289–300. http://www.jstor.org/stable/2346101.

[42] T. Anderlei, W. Zang, M. Papaspyrou, J. Büchs, Online respiration activity

measurement (OTR, CTR, RQ) in shake flasks, Biochem. Eng. J. 17 (2004) 187–194. doi:https://doi.org/10.1016/S1369-703X(03)00181-5.

[43] C. Lui, J. Lievense, Lactic acid producing yeast - US Patent application 20050112737, 2005.

[44] A. Pacheco, G. Talaia, J. Sa-Pessoa, D. Bessa, M.J. Goncalves, R. Moreira, S. Paiva, M. Casal, O. Queiros, Lactic acid production in Saccharomyces cerevisiae is modulated by expression of the monocarboxylate transporters Jen1 and Ady2., FEMS Yeast Res. 12 (2012) 375–381. doi:10.1111/j.1567-1364.2012.00790.x.

[45] A.K. Gombert, M. Moreira dos Santos, B. Christensen, J. Nielsen, Network Identification and Flux Quantification in the Central Metabolism of Saccharomyces cerevisiae under Different Conditions of Glucose Repression, J. Bacteriol. . 183 (2001) 1441–1451. http://jb.asm.org/content/183/4/1441.abstract.

[46] H. Maaheimo, J. Fiaux, Z.P. Cakar, J.E. Bailey, U. Sauer, T. Szyperski, Central carbon metabolism of Saccharomyces cerevisiae explored by biosynthetic fractional (13)C labeling of common amino acids., Eur. J. Biochem. 268 (2001) 2464–2479.

[47] K.R. Kildegaard, B.M. Hallstrom, T.H. Blicher, N. Sonnenschein, N.B. Jensen, S. Sherstyk, S.J. Harrison, J. Maury, M.J. Herrgard, A.S. Juncker, J. Forster, J. Nielsen, I. Borodina, Evolution reveals a glutathione-dependent mechanism of 3-hydroxypropionic acid tolerance., Metab. Eng. 26 (2014) 57–66. doi:10.1016/j.ymben.2014.09.004.

[48] M.P. Dalwadi, J.R. King, N.P. Minton, Multi-timescale analysis of a metabolic

network in synthetic biology: a kinetic model for 3-hydroxypropionic acid production via beta-alanine, J. Math. Biol. (2017). doi:10.1007/s00285-017-1189-3.

[49] K.-S. Kim, J.G. Pelton, W.B. Inwood, U. Andersen, S. Kustu, D.E. Wemmer, The Rut pathway for pyrimidine degradation: novel chemistry and toxicity problems., J. Bacteriol. 192 (2010) 4089–4102. doi:10.1128/JB.00201-10.

[50] E.K.R. Hanko, N.P. Minton, N. Malys, Characterisation of a 3-hydroxypropionic acid-inducible system from Pseudomonas putida for orthogonal gene expression control in Escherichia coli and Cupriavidus necator, Sci. Rep. 7 (2017) 1724. doi:10.1038/s41598-017-01850-w.

[51] J.K. Rogers, G.M. Church, Genetically encoded sensors enable real-time observation of metabolite production, Proc. Natl. Acad. Sci. . 113 (2016) 2388–2393. http://www.pnas.org/content/113/9/2388.abstract.

Table 1. Fermentation parameters of Crabtree-negative, hydroxy acid producing strains under batch conditions[a].

Strain	STtam_2803	STlac_7031	STmal_5413	SThpdh_2779	SThibadh_2780
Description	Parental TAM strain	Lactate producer	Malate Producer	3HP producer (HPDH)	3HP producer (HIBADH)
Max Product Titre (g L^{-1})	16.5±0.1	30.2±2.2	26.8±0.3	3.7±0.1	3.4±0.2
Product Yield (mol mol^{-1} glucose)	0.340±0.004	0.600±0.091	0.363±0.010	0.070±0.005	0.067±0.007
Final OD_{600}	63.9±2.2	86.2±2.4	58.6±2.2	51.6±0.5	56.5±1.6
Maximum specific growth rate (h^{-1})	0.057±0.004	0.094±0.016	0.058±0.003	0.056±0.008	0.057±0.002
Succinate (g L^{-1})	0.17±0.06	0.42±0.02	3.97±0.08	0.70±0.06	0.91±0.09
Glycerol (g L^{-1})	6.00±0.05	0.25±0.01	2.54±0.06	2.07±0.20	2.93±0.18

[a] These parameters were measured in shake flask fermentations in mineral media containing 100 g L^{-1} initial glucose concentration and supplemented with 50 g L^{-1} $CaCO_3$. Metabolite concentrations were analysed by HPLC, except for malate, which was measured by enzymatic assay. Pyruvate concentration could not be quantified by HPLC for the engineered strains.

Figures

Figure 1. Metabolic routes for the production of three different hydroxy acids in Crabtree-negative *S. cerevisiae*. Lactate (A), malate (B), and 3HP (C) are produced from pyruvate in the PDC-negative, pyruvate overproducing host strain (TAM strain – STtam_2803) through the implementation of heterologous pathways. Enzymes required for each step are shown in the oval boxes. Enzyme abbreviations; L-LDH – L-lactate dehydrogenase, PYC – pyruvate carboxylase, MDH – malate dehydrogenase, MAE – malate transporter, AAT – aspartate amino transferase, PAND – aspartate decarboxylase, BAPAT – β-alanine pyruvate amino transferase, HIBADH – 3-hydroxyisobutarate dehydrogenase (NADH-dependent), HPDH – 3-hydroxypropionic acid dehydrogenase (NADPH-dependent. Metabolite abbreviations; 3HP – 3-hydroxypropionic acid. Details about strain construction can be found in the methods section of this article.

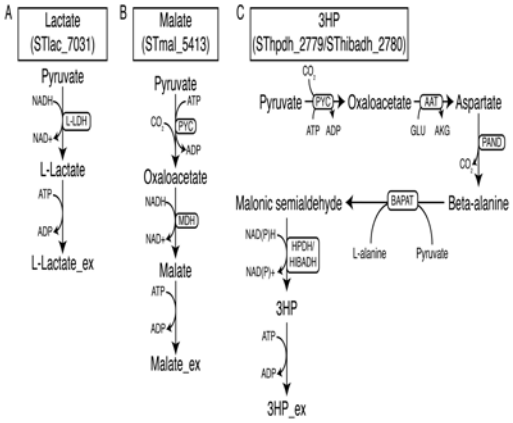

Figure 2. Fermentation profiles of the hydroxy acid production strains. Time-course fermentations with 100 g L^{-1} initial glucose concentrations showing a) STtam_2803 - parental TAM strain, b) STlac_7031 - TAM strain with lactate production pathway, c) STmal_5413 - TAM strain with malate production pathway, d) SThpdh_2779 - TAM strain with HPDH-dependent 3HP pathway, e) SThibadh_2780 - TAM strain with HIBADH-dependent 3HP pathway. Each fermentation was run for 120 hrs and in triplicate. Metabolite concentrations were analysed by HPLC, except for malate, which was measured by enzymatic assay. Pyruvate concentration could not be quantified by HPLC for the engineered strains. Values shown are the mean average for each time point ± SD.

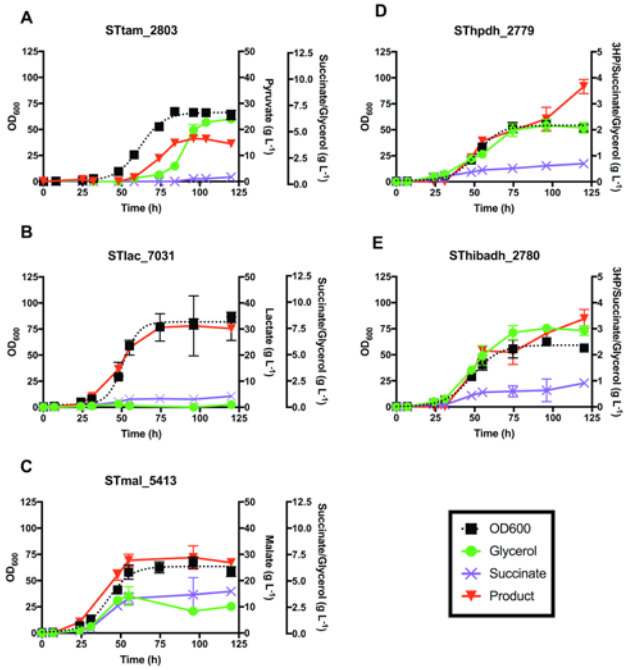

Figure 3. ^{13}C-based metabolic flux and transcriptomic analyses of central carbon metabolism of the hydroxy acid production strains under batch fermentation conditions with 10 g L^{-1} initial glucose concentrations. Crabtree-negative *S. cerevisiae* strains (TAM – STtam_2803) producing different hydroxy acids; lactate (STlac_7031), malate (STmal_5413), and 3HP (SThpdh_2779 and SThibadh_2780) were analysed for their relative flux distributions and the differential expression of the genes involved in each reaction. Bar charts next to each reaction show the relative flux values for each strain calculated from a genome scale model constrained with data from ^{13}C-MFA (normalised over glucose uptake rate). Underneath each graph are heat map plots for the relative transcript levels. Beside each heat map plot is the name of the associated gene. GLC glucose, G6P glucose-6-phosphate, 6PGL D-6-phospho-glucono-δ-lactone, 6PGC 6-phospho-D-gluconate, RU5P ribulose-5-phosphate, XU5P xylulose-5-phosphate, R5P ribose-5-phosphate, S7P sedoheptulose-7-phosphate, G3P glyceraldehyde-3-phosphate, E4P erythrose-4-phosphate, F6P fructose-6-phosphate, FDP fructose-1,6-diphosphate, DHAP dihydroxy-acetone-phosphate, GLYC3P glycerol-3-phosphate, GLYC glycerol, 13DPG 1,3-diphosphateglycerate, 3PG 3-phosphoglycerate, 2PG 2-phosphoglycerate, PEP phosphoenolpyruvate, PYRcyt pyruvate (cytosolic), ACALD acetaldehyde, EtOH ethanol, AC acetate, PYRmit pyruvate (mitochondrial), ACoAmit acetyl-CoA (mitochondrial), CIT citrate, ICIT isocitrate, AKG α-ketoglutarate, SUCCoA succinyl-CoA, SUC succinate, FUM fumarate, MAL malate, OAA oxaloacetate.

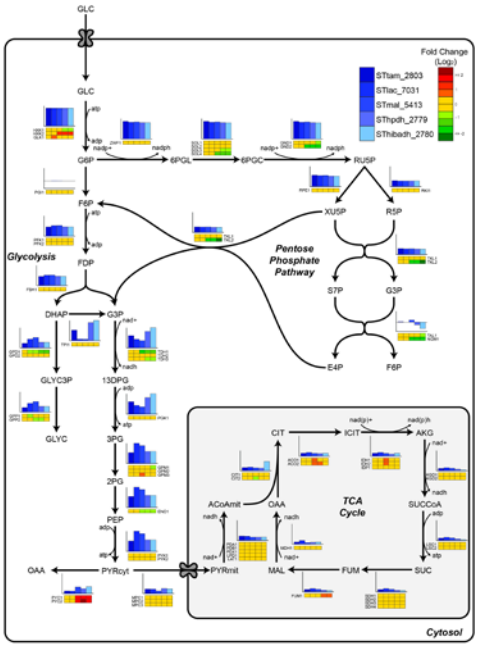

Figure 4. Principle component analysis of the transcriptomic profiles of Crabtree-negative hydroxy acid production strains. Each point represents a single biological replicate, while colour denotes strain identity. The contours of the same colour represent the 95% confidence bounds for each strain. PC – principle component.